Nanoscale

Accepted Manuscript

This article can be cited before page numbers have been issued, to do this please use: G. Torrieri, F. Fontana, P. Figueiredo, Z. Liu, M. Ferreira, V. Talman, J. P. Martins, M. Fusciello, K. Moslova, T. teesalu, V. Ceullo, J. Hirvonen, H. Ruskoaho, V. Balasubramanian and H. A. Santos, *Nanoscale*, 2020, DOI: 10.1039/C9NR09934D.

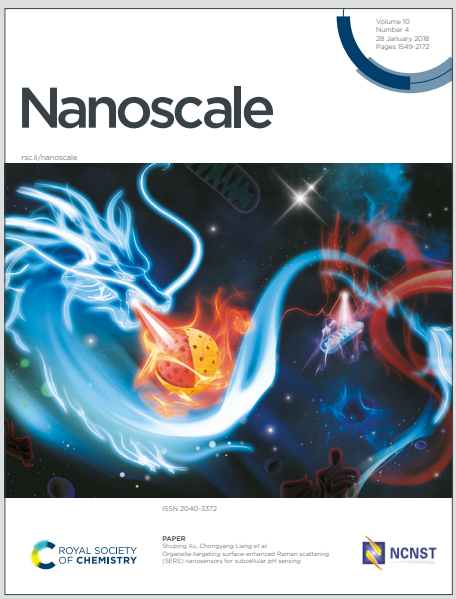

ROYAL SOCIETY OF CHEMISTRY

rsc.li/nanoscale

View Article Online
DOI: 10.1039/C9NR09934D

COMMUNICATION

Dual-Peptide Functionalized Acetalated Dextran-Based Nanoparticles for Sequential Targeting of Macrophages during Myocardial Infarction

Received 00th January 20xx,
Accepted 00th January 20xx

DOI: 10.1039/x0xx00000x

Giulia Torrieri[a], Flavia Fontana[a], Patrícia Figueiredo[a], Zehua Liu[a], Mónica P. A. Ferreira[a], Virpi Talman[b,c], João P. Martins[a], Manlio Fusciello[d], Karina Moslova[e], Tambet Teesalu[f,g], Vincenzo Cerullo[d,h], Jouni Hirvonen[a], Heikki Ruskoaho[b], Vimalkumar Balasubramanian[a]*, Hélder A. Santos[a,h]*

The advent of nanomedicine has recently started to innovate the treatment of cardiovascular diseases, in particular myocardial infarction. Although current approaches are very promising, there is still urgent need for advanced targeting strategies. In this work, the exploitation of macrophages recruitment is proposed as novel and synergistic approach to improve the addressability of the infarcted myocardium achieved by current peptide-based heart targeting. For this purpose, an acetalated dextran-based nanosystem is designed and successfully functionalized with two different peptides, atrial natriuretic peptide (ANP) and linTT1, which are targeting, respectively, cardiac cells and macrophages associated to the atherosclerotic plaques. Biocompatibility of the nanocarrier is screened on both macrophages cell lines and primary macrophages, showing high safety, in particular after functionalization of the nanoparticles' surface. Furthermore, the system shows higher association versus uptake ratio towards M2–like macrophages (approximately 2–fold and 6–fold increase in murine and human primary M2–like macrophages, respectively, compared to M1–like). Overall, the results demonstrate that the nanosystem has a potential ability to exploit the "hitchhike" effect on M2–like macrophages and potentially improve, in a dual targeting strategy, the ability of ANP peptide to target the infarcted heart.

1. Introduction

Cardiovascular diseases (CVDs), and in particular, myocardial infarction (MI), are a global burden, causing 17.8 million deaths in 2017.[1] The high mortality associated with CVDs is due to the inability of human adult heart to replace the loss of cardiomyocytes (up to one billion may be lost in a MI)[2] and restore the cardiac function.[3] Fibrosis is taking place instead, leading to a chronic lethal syndrome, called heart failure (HF).[4] Unfortunately, current therapies are still unsuccessful, because they are mainly aimed at managing symptoms of the disease, but unable to change the fate of cardiomyocytes.

The advent of nanomedicine has brought new insights in innovative treatment strategies, currently at the pre-clinical stage, of CVD, in particular MI.[5–10] Such approaches are very promising, but there is urgent need for smart targeting strategies. The infarcted tissue is challenging to address due to mechanical obstacles, like the constant pumping of the organ and the restless massive exchange of blood.[11] Recently, Ferreira et al.,[12] investigated the in vivo targeting abilities of different heart targeting peptides, demonstrating that atrial natriuretic peptide (ANP) is a peptide that allows nanoparticles to accumulate in the infarcted heart. However, ANP lacks of targeting exclusiveness towards the cardiac tissue, because its receptors are expressed not only in the heart, but also in the kidneys, lungs, brain, testis, adipose tissue, adrenal gland tissues and vascular smooth muscle cells.[13] Herein, we introduce an alternative strategy to improve the heart targeting properties of ANP. Considering the conspicuous involvement of inflammation during infarction, we explore the macrophage recruitment in order to "hitchhike" on macrophages and increase the ANP-functionalized nanoparticles accumulation in the infarcted heart. It is known that promptly after MI, neutrophils are recruited to the infarcted tissue, creating an oxidative stress milieu and producing a variety of inflammatory cytokines, which will further recruit on-site different

[a] Drug Research Program, Division of Pharmaceutical Chemistry and Technology, Faculty of Pharmacy, University of Helsinki, FI-00014 Helsinki, Finland
[b] Drug Research Program, Division of Pharmacology and Pharmacotherapy, Faculty of Pharmacy, University of Helsinki, FI-00140, Helsinki, Finland
[c] National Heart and Lung Institute, Imperial College London, London W12 0NN, United Kingdom
[d] Drug Research Program, Division of Pharmaceutical Biosciences, Faculty of Pharmacy, University of Helsinki, FI-00140, Helsinki, Finland
[e] Department of Chemistry, University of Helsinki, FI-00014, Helsinki, Finland
[f] Laboratory of Cancer Biology, Institute of Biomedicine and Translational Medicine, Centre of Excellence for Translational Medicine, University of Tartu, Tartu, 50411, Estonia
[g] Cancer Research Center, Sanford-Burnham Medical Research Institute, La Jolla, California 92037, USA
[h] Helsinki Institute of Life Science, HiLIFE, University of Helsinki, FI-00014 Helsinki, Finland
* E-mail: vimalkumar.balasubramanian@helsinki.fi; helder.santos@helsinki.fi

† Electronic Supplementary Information (ESI) available: [details of any supplementary information available should be included here]. See DOI: 10.1039/x0xx00000x

View Article Online
DOI: 10.1039/C9NR09074D

populations of monocytes and macrophages.[14,15] This monocytes/macrophages enrolment can be divided into two sequential phases. A first phase, which peaks at day 3 after the onset of MI, sees an accumulation of inflammatory type Ly-6C^{high} monocytes / M1–type macrophages, which phagocytose dead cells and debris to make space for the evolving scar. Six days after the infarction onset, a second phase, characterized by the presence of healing Ly-6C$^{int/low}$ monocytes / M2–type macrophages, supervenes and promotes the repair of the tissue with release of vascular endothelial growth factor (VEGF) and transforming growth factor beta (TGFβ), which are supporting angiogenesis and collagen production, leading to formation of un-functional scar tissue.[14,15]

Cellular hitchhiking is a very well-known approach used in the nanomedicine field.[16] In the past, researchers exploited the long circulating properties of red blood cells,[17,18] macrophages/monocytes[19–22] and other cells[23,24] to increase the circulation time[17] and targeting abilities of specific nanocarriers,[18] and avoid the rapid clearance of diagnostic and imaging agents.[22] With this aim, we designed a putrescine-modified acetalated dextran (Putre-AcDEX)-based nanosystem, functionalized with ANP and TT1 peptides

Acetalated dextran (AcDEX) was chosen because it is easy to modify, highly biocompatible both as starting material and in terms of degradation products,[25] and due to its pH-responsiveness.[26,27] The polymer was modified with putrescine to provide functional groups for further surface conjugations and to reduce the toxicity towards primary cardiomyocytes observed with spermine-modified nanoparticles.[5] Spermine particles are highly positive charged even after the conjugations, due to free amine groups present in the structure. The system was loaded with two small hydrophobic compounds, CHIR99021 and SB203580, which have shown synergistic effect in stimulating cardiomyocyte proliferation.[28]

To endow nanoparticles with heart targeting ability, the surface of the nanocarrier was modified with ANP and TT1 peptides, attached to the nanoparticles' surface through a branched polyethylene glycol (PEG). Linear TT1 (Lin-TT1) (AKRGARSTA) is a well-established peptide for its tumor-homing abilities.[29–31] The peptide addresses tumors by binding to the mitochondrial chaperone protein p32, normally expressed at intracellular level, but translocated on the surface of tumor cells, tumor associated macrophages, tumor endothelial cells, as well as on macrophages associated with atherosclerotic plaques.[30,32,33] TT1 peptide, similarly to integrin-binding arginine-glycine-aspartic acid (iRGD) and LyP-1 peptides, contains a cryptic basic sequence motif (C-end Rule or CendR motif), that is, following cell surface recruitment of the peptide by p32-dependent mechanism, proteolytically processed to activate CendR element and allow interaction of the peptide with the secondary receptor neutropilin-1 (NRP-1).[34] This interaction initiates an uptake process similar to classical endocytosis.[34]

The aim of this work was to evaluate the successful conjugation of both peptide moieties on the nanoparticles' surface, assessing the biocompatibility of the nanosystem and studying its interactions with both continuous macrophages cell lines and primary M1– and M2–like macrophages. For this purpose, we have tested viability and uptake of both macrophages cell lines and primary macrophages treated with different concentrations of the nanosystem.

2. Results and discussions

2.1. Characterization of Putre-AcDEX Nanoparticles

Putre-AcDEX nanoparticles were prepared by an oil-in-water (o/w) single emulsion method.[35] The two hydrophobic compounds, CHIR99021 and SB203580 (abbreviated as C and S, respectively) were dissolved together with the polymer in the organic phase. Then, an aqueous solution of polyvinyl alcohol (PVA), which functions as stabilizer, was added and the emulsion was created with the help of high energy sonication. Upon evaporation of the organic solvent for 3h, the nanoparticles formed entrapped the compounds in a matrix-like structure. The surface of the nanoparticles was then functionalized with PEG and the two peptides, linTT1 and ANP, in order to achieve dual targeting. After preparation, the nanoparticles were characterized by dynamic light scattering (DLS) and electrophoretic light scattering (ELS) to obtain information about their size, polydispersity index (PDI), and zeta (ζ)-potential (Figure 1A).

The nanoparticles were characterized by increase of size after different conjugation steps. In particular, empty nanosystems showed a significant increase in hydrodynamic diameter after functionalization with the two peptides. Loaded particles did not show such size increase, suggesting a stabilizing effect of the loaded compounds, C and S.

The PDI varied accordingly, showing higher values for empty particles after conjugation with linTT1 and ANP peptides, which are characteristic of heterogeneous nanoparticles suspensions,[36] supporting the stabilizing theory of the loaded compounds. The charge of the nanoparticles was also measured, suggesting that the different components were effectively conjugated on the surface of the nanoparticles. The bare nanosystem had a high positive charge (ca. +40 mV), due to the presence of amine groups from putrescine. After PEGylation, the ζ-potential dropped to negative values (−30 mV), due to the presence of carboxyl-terminated groups in the PEG. The conjugation of linTT1 peptide, reversed the charge to slightly positive values (ca. +10 mV), and this can be explained due to the presence of arginine residues in the peptide sequence. The charge had a further small increase of ca. 10 mV (reaching values of +20 mV) after conjugation of ANP peptide, which is rich of positively charged arginine residues, and thus, responsible for the increase of the positive charge. The presence of PEG was furthermore confirmed by KBr−Fourier transform infrared (FTIR) spectroscopy (Figure 1B).

The presence of the of amide–indicative bands at 1565–1570 cm^{-1} (in-plane N–H bending and C–N stretching) and 1630–1640 cm^{-1} (amide C=O stretching) confirmed the formation of a covalent amide bond between the Putre-AcDEX and PEG, and the appearance of a shoulder at 1735 cm^{-1} (C=O stretching from –COOH belonging to PEG and maleimide groups,

View Article Online
DOI: 10.1039/C9NR09934D

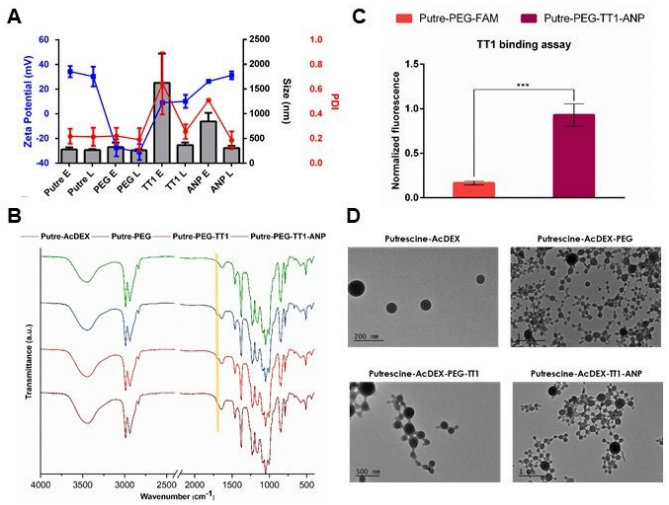

Figure 1. Physicochemical characterization of Putre-AcDEX nanoparticles. (A) Average size, PDI, and ζ-potential before and after the different conjugation steps. Letters E and L are used to differentiate between empty and loaded particles, respectively. Bare system is named as Putre; PEGylated nanoparticles are abbreviated as PEG; particles conjugated with only TT1 peptide are named as TT1, and the system after conjugation with all the peptides is called ANP. (B) KBr–FTIR spectra of the bare and functionalized nanoparticles. (C) TT1 binding assay. Fluorescent labelled nanoparticles conjugated with both ANP and TT1 peptides (Putre-PEG-TT1-ANP) were compared with PEGylated particles made fluorescent after conjugation with 6-Carboxyfluorescein (Putre-PEG-FAM) (D) TEM images of the bare nanoparticles and after surface functionalization. Values are represented as the mean ± standard deviation (s.d.) (n ≥ 3 biological replicates in which each time 3 technical replicates have been used). The data were analysed by two-way ANOVA followed by a Tukey–Kramer post hoc test, using GraphPad Prism 7 software. Statistical significance was set at probabilities of *p < 0.05, **p < 0.01, and ***p < 0.001.

underlined by the yellow band in Figure 1B, denotes the presence of free carboxyl groups.

The conjugation of linTT1 and ANP peptides did not change the FTIR spectrum, thus further methods were used to confirm the successful conjugation of the peptides onto the nanoparticle's surface. LinTT1 presence was detectable due to its conjugation with carboxyfluorescein (FAM), which imparted fluorescence to the nanoparticles after conjugation with the peptide. Moreover, we performed a binding assay to ensure that the peptide was conjugated with correct orientation, and thus, kept its functionality. The assay consisted in coating Ni-NTA magnetic agarose beads with recombinant hexahistidine-tagged target of linTT1 peptide, p32.[37] Then, beads were incubated with FAM-labeled nanoparticles conjugated with the linTT1peptide or without it. Beads were finally washed the nanoparticle-p32 complexes were released using imidazole elution buffer and the eluted fluorescence was measured. As shown in Figure 1C, the eluted fractions collected from beads incubated with Putre-PEG-TT1-ANP nanoparticles, presented a significantly higher fluorescence compared to those collected from beads that interacted with particles without peptide. This demonstrates that functionally active linTT1 peptide was conjugated onto the nanoparticles' surface. The effective conjugation of ANP was further confirmed by elemental analysis, which showed the presence of about 14.14 µg of ANP in 1 mg of Putre-PEG-TT1-ANP nanoparticles (Table S2).

The nanoparticles' morphology was observed through transmission electron microscopy (TEM) images (Figure 1D), which showed round-shaped nanoparticles, with diameter comprised between 100 and 200 nm, a bit smaller than what was observed with DLS. This phenomenon is in accordance to the fact that DLS measures the hydrodynamic diameter of the particles, whereas TEM refers to dry particles.[38]

2.2. Release Studies and pH-Dependent Behavior

The release profile of the two encapsulated drug compounds, C and S, was evaluated in phosphate buffer saline (PBS) (pH 7.4) and acetate (pH 5.0) buffers, in order to mimic the physiological extracellular environment and the conditions found in acidic intracellular compartments after internalization in the cells, respectively.[39] In addition, the determination of the drug loading degree (LD) and encapsulation efficiency (EE) values of bare and functionalized particles were also conducted as shown in Table S3.

The encapsulation of the drug molecules was done at a molar ratio C:S of 1:2, which is the optimal ratio, according to literature, in order to induce cardiomyocytes proliferation.[40,41] Upon functionalization, there is loss of encapsulated drugs, because some of the compounds might still be on the surface of the nanoparticles, even though they were washed

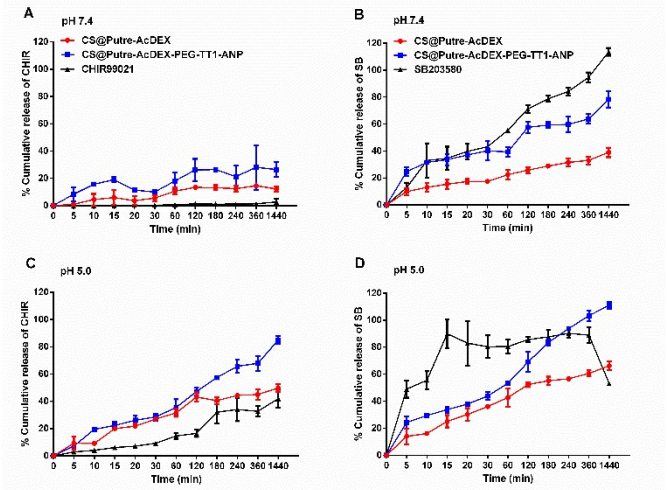

Figure 2. Release profiles of drug-loaded Putre-AcDEX nanoparticles. Release profiles of CHIR99021 (A and C) and SB203580 (B and D) from bare CS@Putre-AcDEX and functionalized CS@Putre-AcDEX-PEG-TT1-ANP at pH 7.4 and 5.0, at 37 °C. Data represented as mean ± s.d. (n ≥ 3 biological replicates in which each time 3 technical replicates have been used).

thoroughly. Another reason could be that the system is saturated due to the
high amount of compounds loaded at the beginning of the preparation process.
However, the amount of encapsulated drugs was still enough to produce an effect on cells.[42,43]
As previously demonstrated,[44–46] AcDEX-based nanoparticles should release drugs faster at acidic pH, because of the pH-dependent hydrolysis of acetal groups present in AcDEX. Results obtained are in accordance with what was previously reported, as shown in Figure 2.
At pH 5.0 both the drugs were released faster compared to pH 7.4 (Figure 2C and 2D). Free drugs were used as controls and especially in the case of C, nanoparticles increased its dissolution rate in aqueous media. Also, the solubility of C was affected by the pH, where the free drug was more soluble at pH 5.0 than at pH 7.4. For S at pH 5.0, it can be noticed the nanoparticles prevented drug degradation, because the free drug started degrading after 8h, whereas the drug-loaded nanoparticles showed release of the drug concentration up to 24h. Moreover, the nanosystem conjugated with PEG and the peptides (named CS@Putre-AcDEX-PEG-TT1-ANP in the plot), presented a faster drug release of the drugs compared to the bare nanoparticles (named CS@Putre-AcDEX in the plot). This can be explained by the increased hydrophilicity of the nanosystem after surface modifications, which can promote the interaction with the solvent molecules and allow the release of the drugs entrapped in the polymer matrix close to the surface of the nanoparticles.[47–49]
Even though the drug release was faster at pH 5.0, there was a small amount of drugs released already at pH 7.4, which is justifiable by a slight degradation of AcDEX at this pH, as previously reported.[5,50] This loss of drugs at pH 7.4 can also justify the decrease of the LD and EE values of the nanoparticles after the various conjugation steps. After PEGylation, washings were performed in a solution of 2% of sucrose at pH 7.4, in order to prevent the degradation of the maleimide groups of PEG needed to interact with the thiol groups of TT1 peptide. Overall, these AcDEX-based nanoparticles were successfully designed to release payloads mostly in the acidic subcellular compartments of the cells, which can be considered optimal for an intravenous administration. Furthermore, it is known that inflammation occurring in the ischemic myocardium lowers the interstitial pH to 6–6.5, which makes the AcDEX-based nanoparticles a valuable candidate for sustained release of cargos in the infarcted heart.[26,27]

2.3. Cytocompatibility

The cytocompatibility of the developed nanosystem was assessed on macrophages cell lines, RAW 264.7 and KG-1, as well as on primary macrophages, of both human and murine origins. Cells were incubated with the nanoparticles for 24 and 48h, since the drugs are released in 24h and also because the desired effect on cardiomyocytes, produced by the compounds C and S (stimulation of cardiomyocytes proliferation by re-entry of cardiomyocytes in the cell cycle), takes time to manifest. At each time point, cell viability was assessed by CellTiter-Glo® luminescence assay.[51] As shown in Figure 3, both bare nanoparticles and Putre-AcDEX-PEG-TT1-ANP, empty and loaded, were safe towards RAW 264.7 and KG-1 cell lines.
Empty bare nanoparticles were slightly toxic at higher concentrations, probably due to the presence of putrescine, which endows the nanosystems with high positive charge. Positively charged nanoparticles are toxic towards cells, because of the high interaction between the cationic surface groups of the nanoparticles and the negatively charged cell membranes, which cause disruption of the plasma-membrane integrity, production of high number of autophagosomes and damage to cellular organelles, in particular mitochondria and lysosomes.[52] After surface functionalization, the charge of the nanosystems is not highly positive anymore, thus the toxicity is reduced and the nanoparticles are more likely biocompatible. Moreover, the encapsulation of drugs corresponded to a significant increase in cell viability, suggesting a protective effect of the two compounds.[53–55] Researchers demonstrated that inhibition of p38 MAPK[53] and activation of canonical wnt signaling[55] pathways are implicated not only in cytokine production of stimulated macrophages, but also in their proliferation. SB203580, a p38 MAPK inhibitor, promotes

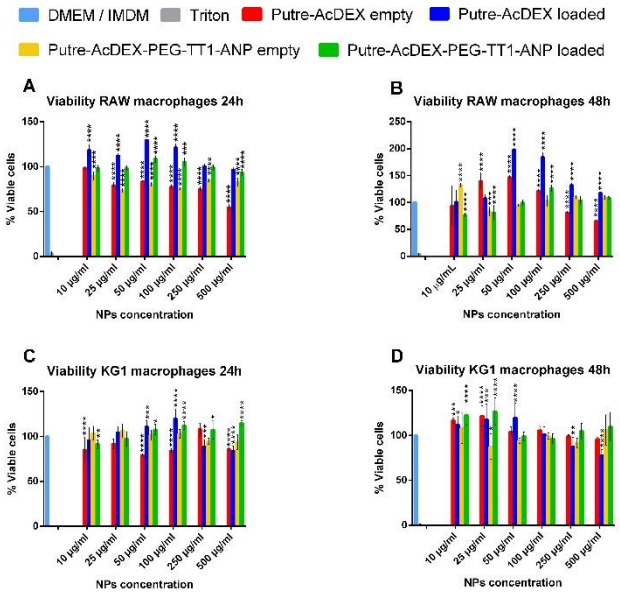

Figure 3. Cell viability of macrophages cells lines. Cytocompatibility studies were conducted to assess the safety of the produced nanoparticles on both RAW 264.7 (A–B) and KG-1 (C–D) cell lines. Values are represented as mean ± s.d. (n = 3 biological replicates in which each time 3 technical replicates have been used). A one-way ANOVA followed by a Tukey–Kramer post hoc test was used for the statistical analysis. The significance levels of the differences were set at probabilities of *p < 0.05, **p < 0.01, ***p < 0.001 and ****p < 0.0001 for comparison with the medium, which was used as control in all the tests.

macrophages proliferation by increasing the stability of

granulocyte-colony stimulating factor (G–CSF) mRNA, and thus, enhancing its expression at post transcriptional level.[53]
Activation of canonical wnt signaling shows proliferative effect through upregulation of cyclin D1 protein expression.[55]
Next, the biocompatibility was also studied in primary macrophages, which showed a higher sensitivity to the positive nature of bare nanoparticles. As shown in Figure 4, the nanoparticles without any surface modification drastically reduced the viability of both M1– and M2–like macrophages, with murine cells being the most sensitive. The cytotoxicity effect was both dose- and time-dependent. Also with primary macrophages, the surface functionalization and the loaded drugs improved the cell biocompatibility of the nanoparticles.

View Article Online
DOI: 10.1039/C9NR09934D

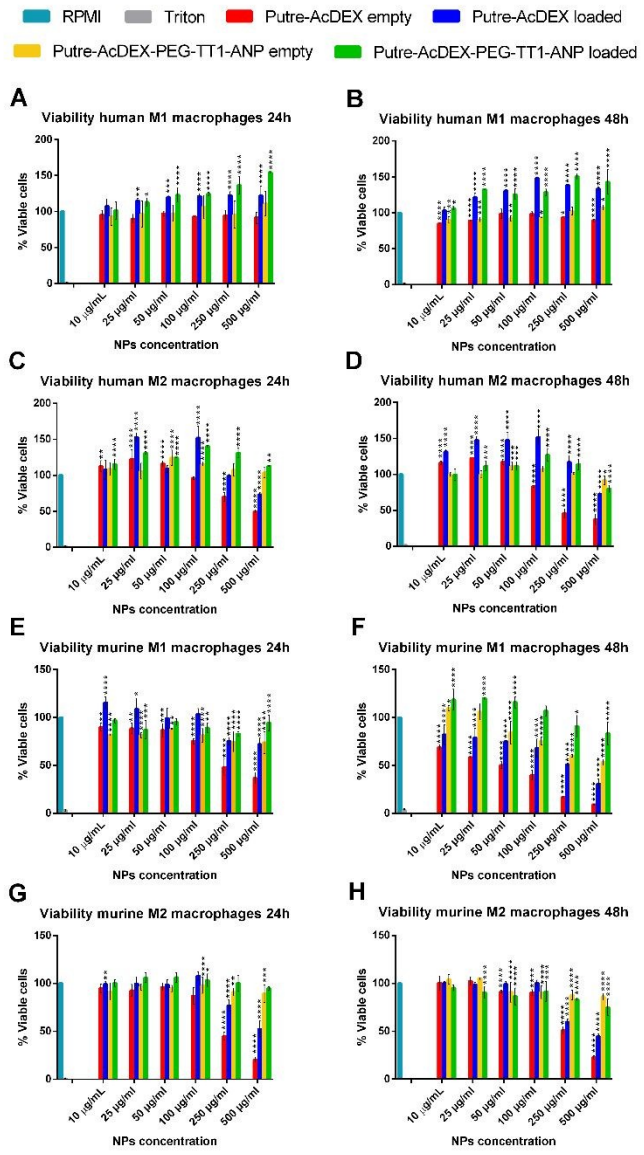

Figure 4. Cytocompatibility of primary macrophages. Cell viability studies on both human (A–D) and murine (E – H) M1– / M2–like macrophages. Biocompatibility was assessed at both 24 (A, C, E, G) and 48h (B, D, F, H). Values are represented as mean ± s.d. (n = 3 biological replicates in which each time 3 technical replicates have been used). A one-way ANOVA followed by a Tukey–Kramer post hoc test was used for the statistical analysis. The significance levels of the differences were set at probabilities of *p < 0.05, **p < 0.01, ***p < 0.001 and ****p < 0.0001 for comparison with the medium, which was used as control in all the tests.

2.4 Cell–Nanoparticle Interactions with Macrophages Cell Lines

Macrophages cell lines, RAW 264.7 and KG-1, were first screened to have preliminary indications on the behavior of the cells in the presence of nanonocarriers. Based on the abovementioned cytocompatibility results, the nanoparticle concentration of 50 µg mL-1 was used in all uptake studies. The cell-nanoparticle interaction was studied by flow cytometry analysis, by incubating the cells for 1h with fluorescently labelled nanoparticles, then washed and prepared for flow cytometry analysis, which was performed by detection of fluorescence of the AlexaFluor488®. Figure 5 shows the median fluorescence intensity (MFI) values for the two cell lines treated with PEGylated and peptides-conjugated nanoparticles. MFI values are proportional to the extent of cell-nanoparticle interaction.
It is known that macrophages express ANP receptors.[56] However, ANP significantly influences uptake properties of macrophages only after a proper incubation time (18h).[56] Thus, in this work we did not study the effect of ANP on different macrophages' uptake profiles.
RAW 264.7 macrophages showed a preferential interaction with Putre-AcDEX-PEG as compared with Putre-AcDEX-PEG-

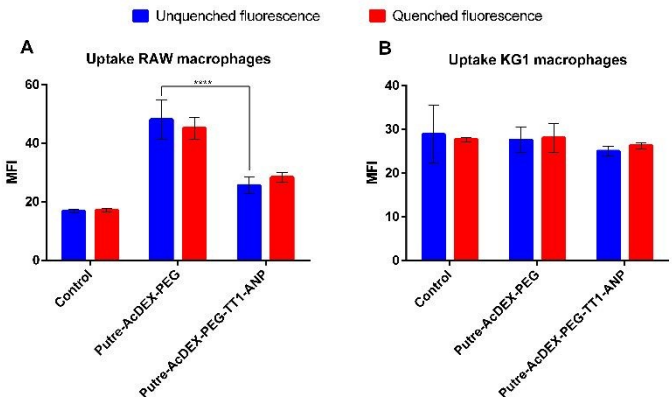

Figure 5. Quantitative uptake studies with macrophages cell lines. Uptake studies have been carried out with both RAW 264.7 (A) and KG-1 (B) cell lines incubated for 1 h with the nanoparticles. Values represent the MFI ± s.d. (n = 3 biological replicates in which each time 3 technical replicates have been used). A one-way ANOVA followed by a Tukey–Kramer post hoc test was used for the statistical analysis. The significance levels of the differences were set at probabilities of ***p < 0.01 for comparison with Putre-AcDEX-PEG and Putre-AcDEX-PEG-TT1-ANP (both before fluorescence quenching with TB), and for Putre-AcDEX-PEG-TT1-ANP, before and after fluorescence quenching.

View Article Online
DOI: 10.1039/C9NR09974D

TT1-ANP. It has been demonstrated that PEGylation improves the "stealth" properties of nanoparticles, and thus, it is expected that PEGylated nanoparticles interact less with cells.[57] However, the internalization rate of PEGylated nanoparticles in this particular case was faster. This can be
explained considering that the PEG attached to the particles had a low number of monomers per chain, and thus, it was expected to be.
internalized faster compared to a PEG with longer chain.[58] In contrast with flow cytometry results, confocal images in Figure S1, showed that particles conjugated with both peptides interacted more with RAW macrophages as compared with the PEGylated nanosystems. Nonetheless, confocal images are only representative of part of the cell population and provide only a qualitative perspective on the interactions between cells and nanoparticles.
KG-1 cells, which are a human non-adherent macrophage cell line, did not show any difference in the interaction between the PEGylated nanosystems and the nanoparticles functionalized with both ANP and TT1 peptides. It is hypothesized that this could be due to the nanoparticles sedimentation over time, excluding themselves from the interaction with the cells.[59]

2.4 Polarization of Human and Murine Monocytes

Monocytes were isolated and collected from human blood and murine bone marrow. After collection, they were maturated and then polarized into M1– and M2–like macrophages by using different cocktails of cytokines (Scheme S1). In order to confirm the impact of our polarization strategies, we assessed the surface expression of a panel of M1 and M2 phenotypic markers (Figures S2 and S3). For both MØ and LPS/IL-4 stimulated macrophages of human origin, CD86 and CD206 were used as M1 and M2 markers, respectively.[60,61] Murine MØ macrophages were recognized by expression of F4/80 and CD11b,[62] whereas M1– and M2–like macrophages, were distinguished by expression of CD206 and CD11c.[63] Unstained cells were used as controls. Before polarization with lipopolysaccharide (LPS), the majority of the human monocytes matured with granulocyte–macrophage colony–stimulating factor (GM–CSF) were $CD206^{+}CD86^{-}$ (Figure S2A). Treatment with LPS shifted the markers expression towards an increase of CD86 positive cells (Figure S2B), thus suggesting that treatment with the cytokine was able to create a population of M1–like macrophages. Similarly, monocytes treated with macrophage colony–stimulating factor (M–CSF), which were double positive for CD206 and CD86 (Figure S2C), showed a shift towards $CD206^{+}CD86^{-}$ upon stimulation with interleukine-4 (IL-4) (Figure S2D). Murine cells exhibited major plasticity compared to human macrophages. Monocytes matured with both GM–CSF and M–CSF were, respectively, $CD11b^{+}F4/80^{-}$ and double positive for F4/80 and CD11b (Figure S3A), typical monocytes markers. Then, LPS stimulated MØ macrophages became $CD11c^{+}CD206^{-}$ macrophages (Figure S3B), whereas the cells treated with IL-4 were double positive (Figure S3D). The cellular morphology also changed depending on the cytokine treatment.

2.5 Cell–Nanoparticle Interactions with Primary Macrophages

Finally, the interactions between the nanoparticles and primary macrophages were also assessed. Previous studies already evaluated the effect of macrophages polarization on nanoparticles uptake, but they obtained contrasting results, depending on the conditions used during the studies and, most importantly, the type on nanoparticles used.[64-66]
Ideally, for intravenous injectable nanosystems and the "hitchhike" effect to the infarcted heart by recruited macrophages to take place, the aim is to obtain a nanosystem that is able to associate with the macrophages' surface, without being taken-up. To understand which type of macrophages was presenting a higher nanoparticle-cell association rate versus uptake, we evaluated the interactions between the hitchhiking nanoparticles and the differentiated M1– and M2–like macrophages derived from both human and murine precursors. Uptake studies were performed as previously done for continuous cell lines.

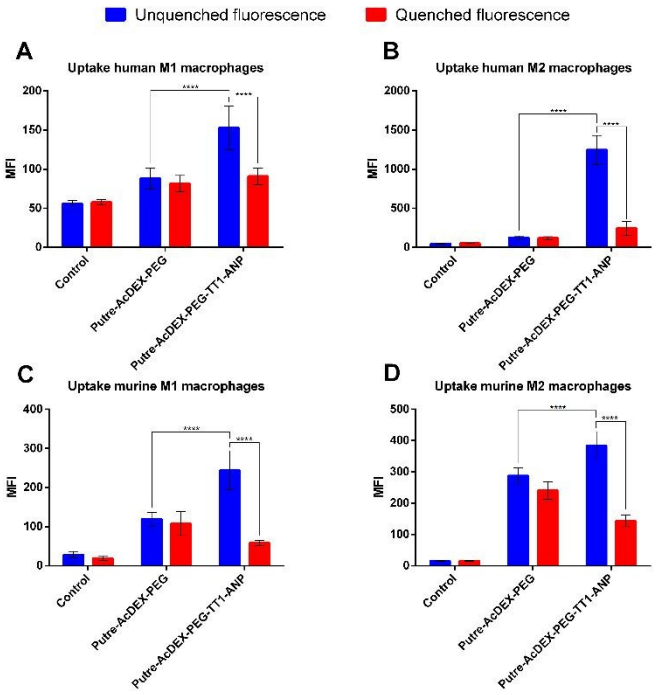

Figure 6. Quantitative cell uptake studies on primary M1 and M2–like macrophages. Interactions between Putre-AcDEX nanoparticles and cells was studied also on human (A, B) and murine (C, D) M1 and M2–like macrophages. Results are represented as MFI values ± s.d. (n = 3 biological replicates in which each time 3 technical replicates have been used). A one-way ANOVA followed by a Tukey–Kramer post hoc test was used for the statistical analysis. The significance levels of the differences were set at probabilities of $*p < 0.05$ and $****p < 0.0001$ for comparison between associated Putre-AcDEX-PEG and the Putre-AcDEX-PEG-TT1-ANP, as well as for internalized Putre-AcDEX-PEG-TT1-ANP, before and after fluorescence quenching with trypan blue.

From the results, we observed that Putre-AcDEX-PEG-TT1-ANP nanoparticles generally interacted more with M2–like macrophages compared to M1–like ones (Figure 6). The nanoparticle-cell association vs uptake ratio was higher for M2–like macrophages in both human and murine cells, suggesting that M2 macrophages can act as more efficient carriers for nanoparticles into the infarcted heart.

Considering these findings and the bi-phasic accumulation of M1– and M2–like macrophages in the infarcted heart, the particles here presented can reach the infarcted heart in an optimal timeframe. The final aim of the designed nanosystem was to induce cardiomyocytes proliferation, restoring the loss of beating cells and cardiac function after infarction. The loaded drugs, C and S, were used for this aim, because it has been shown in the literature that they have a synergic effect in stimulating cardiomyocytes proliferation.[28] In order to be successful in this strategy, we hypothesized that the first phase of macrophages recruitment is needed to phagocytose dead cells and debris, and to make space for the new regenerated tissue.[14] Thus, the ability to exploit the recruitment of M2–like macrophages, suggest an increase of the chances for an optimal tissue remodelling, because the proliferation of cardiomyocytes would contrast the formation of scar tissue.

Results were confirmed also by qualitative cell uptake studies, using florescence confocal microscopy. Different macrophages were incubated with the nanoparticles for 1h and then fixed and stained. Finally, the samples were imaged with an inverted confocal microscope. Images showed that the nanoparticles conjugated with both the peptides interacted more with the cells than the PEGylated ones. Moreover, in the images particles looked green and not yellow, suggesting that the nanoparticles were mainly associated onto the surface of the macrophages, and not taken-up (Figure S4).

Finally, we also studied the mechanism of internalization of Putre-AcDEX-PEG-TT1-ANP nanoparticles. Since we observed higher cell–NP association than cell uptake, especially in M2–like macrophages, we also hypothesized whether the nanoparticles were inducing frustrated endocytosis. For this purpose, NP cell uptake mechanism studies were investigated and quantified as percentage of positive events. Primary macrophages were incubated with different compounds, in order to inhibit particular mechanisms of cell internalization. Cytochalasin D (CytoD) was used at two different concentrations to study the micropinocytosis and the role of actin in the endocytic process, because it is able to depolarize actin filaments.[67,68] Nocodazole was used as a microtubule disruptor,[69,70] in order to assess the influence of microtubules on the nanoparticle internalization. Genistein is an isoflavone used to inhibit caveoline-mediated endocytosis as a result of its suppressive effect on tyrosine kinases involved in this type of internalization.[70–72] Clathrin-mediated uptake was inhibited by Chlorpromazine, which interferes with clathrin disassembly and receptor recycling to the plasma membrane.[73] Sodium azide was used to study whether the particles were taken-up by active transport or not, because it interferes with ATP production due to its ability in inhibiting cytochrome c oxidase.[74,75] Adsorptive-mediated uptake was inhibited by protamine sulphate.[76] All primary macrophages internalized the nanoparticles preferentially by macropynocytosis, as shown in Figure 7.

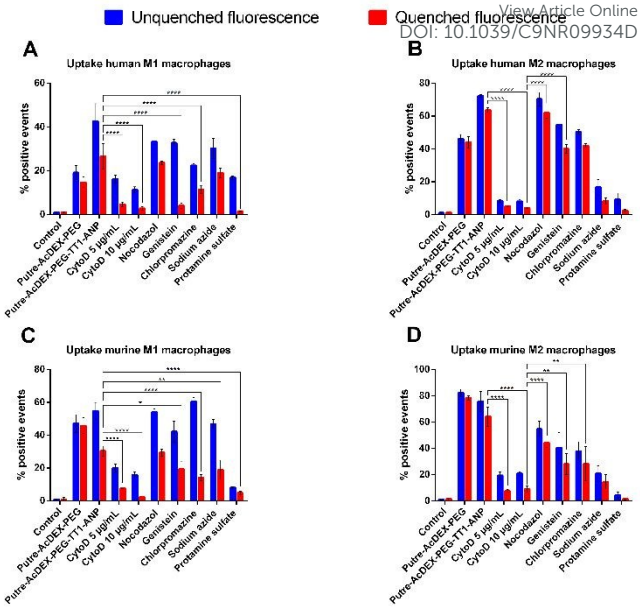

Figure 7. Study of the cell uptake mechanisms. Primary macrophages were incubated with different compounds, each one inhibiting a different mechanism of endocytosis, and then particles were added and the cell uptake evaluated by flow cytometry. Values represent the percentage of positive events ± s.d. (n = 3 biological replicates in which each time 3 technical replicates have been used). A one-way ANOVA followed by a Tukey–Kramer post hoc test was used for the statistical analysis. The significance levels of the differences were set at probabilities of *p < 0.1, ** p < 0.01, *** p < 0.001 and **** p < 0.0001.

Macrophages treated with Cyto D presented the lower values of percentage of positive events for nanoparticles taken-up as compared, for example, to Genistein and Chlorpromazine, which are inhibiting caveoline-mediated endocytosis and clathrin-mediated uptake, respectively. Human derived macrophages (Figure 7A and 7B) had the lowest sensitivity to uptake inhibitors compared to murine cells (Figure 7C and 7D). Also, it was notable that actin filaments, but not microtubules, were the cytoskeleton components involved in the uptake mechanism of the Putre-AcDEX-PEG-TT1-ANP nanoparticles. All these findings suggest the engagement of energy dependent pathways in the endocytosis of the produced nanoparticles, justifying the high association versus cell uptake observed in Figure 6.

Conclusions

Herein, we report the design of a nanocarrier successfully decorated with two different peptides, TT1 and ANP, with

promising targeting ability towards the infarcted heart tissue, through exploitation of macrophages recruitment. Putre-AcDEX nanoparticles after surface modifications were biocompatible towards both macrophages cell lines and primary macrophages of human and murine origin. Moreover, they showed preferential association versus uptake with M2–like macrophages (approximately 2–fold and 6–fold increase in murine and human primary macrophages, respectively, compared to M1–like), which makes them suitable candidates for achieving the "hitchhike" effect and target the infarcted heart in the later stage of the inflammatory response. Overall, the nanosystem developed here has the potential ability to exploit the post-infarction recruitment of M2–like macrophages, to provide new targeting strategies in the field of nanomedicines for heart disease treatment.

Ethical statement

All experimental protocols with animals were approved by the Laboratory Animal Center of the University of Helsinki and the National Animal Experiment Board of Finland according to the EU's Guidelines for Accommodation and Care of Animals, following the Act (497/2013) and the Decree (564/2013) on Animal Experimentation approved by the Finnish Ministry of Agriculture and Forestry, and the EU Directive (2010/63/EU). For the primary cell cultures for *in vitro* experiments the animals were used after an internal license was authorized and approved by the Laboratory Animal Centre, University of Helsinki (Finland). All human blood samples were purchased from the Finnish Red Cross Blood Service (Veripalvelu) obtained from anonymous donors.

Conflicts of interest

Authors declare no conflict of interest.

Acknowledgements

Dr. A. Rahikkala is acknowledged for providing protocols for PBMCs isolation. Dr. W. Li is acknowledged for helping with KBr-FTIR. Dr. V. Balasubramanian acknowledges University of Helsinki Research Funds. Prof. Hélder A. Santos acknowledges financial support from the HiLIFE Research Funds, the Sigrid Jusélius Foundation and the Academy of Finland (grant no. 317042). T. Teesalu was supported by the European Union through the European Regional Development Fund (Project No. 2014-2020.4.01.15-0012) and by European Research Council grant GlioGuide from European Regional Development Fund. The authors also acknowledge the following core facilities funded by Biocenter Finland: Electron Microscopy Unity of the University for providing the facilities for TEM imaging, Flow cytometry, MST and Biacore core facilities of the University for the flow cytometer and the Light Microscopy Unit of the Institute of Biotechnology for the confocal microscope.

References

1 G. A. Roth, D. Abate, K. H. Abate et al., *Lancet*, 2018, 392, 1736.
2 M. A. Laflamme, C. E. Murry, *Nat. Biotechnol.*, 2005, 23, 845.
3 A. Uygur, R. T. Lee, *Dev. Cell.*, 2016, 36, 362.
4 V. Talman, H. Ruskoaho, *Cell Tissue Res.*, 2016, 365, 563.
5 M. P. A. Ferreira, V. Talman, G. Torrieri et al., *Adv. Funct. Mater.*, 2018, 28, 1705134.
6 R. C. Scott, J. M. Rosano, Z. Ivanov et al., *FASEB J.*, 2009, 23, 3361.
7 J. Park, B. Kim, J. Han et al., *ACS Nano.*, 2015, 9, 4987.
8 Y. Chang, E. Lee, J. Kim et al., *Biomaterials*, 2019, 192, 500.
9 Z. Fan, Z. Xu, H. Niu et al., *J. Control. Release*, 2019, DOI: 10.1016/j.jconrel.2019.09.005.
10 M. P. A. Ferreira, S. Ranjan, S. Kinnunen et al., *Small*, 2017, 13,1701276.
11 M. Shin, H. -A. Lee, M. Lee et al., *Nat. Biomed. Eng.*, 2018, 2, 304.
12 M. P. A. Ferreira, S. Ranjan, A. M. R. Correia et al., *Biomaterials*, 2016, 94, 93.
13 L. R. Potter, A. R. Yoder, D. R. Flora et al., *Exp. Pharmacol.*, 2009, 191, 341.
14 M. Nahrendorf, F. K. Swirski, E. Aikawa et al., *J. Exp. Med.*, 2007, 204, 3037.
15 M. Nahrendorf, F. K. Swirski, *Circ. Res.*, 2013, 112, 1624–1633.
16 A. C. Anselmo, S. Mitragotri, *J. Control. Release*, 2014, 190, 531.
17 E. Chambers, S. Mitragotri, *J. Control. Release*, 2004, 100, 111.
18 A. C. Anselmo, V. Gupta, B. J. Zern et al., *ACS Nano*, 2013, 7, 11129.
19 A. M. Brynskikh, Y. Zhao, R. L. Mosley et al., *Nanomedicine (Lond).*, 2010, 5, 379.
20 H. Dou, C. B. Grotepas, J. M. McMillan et al., J. Immunol. 2009, 183, 661.
21 M. -R. Choi, R. Bardhan, K. J. Stanton-Maxey et al., *Cancer Nanotechnol.*, 2012, 3, 47.
22 J. Choi, H. -Y. Kim, E. J. Ju et al., Biomaterials, 2012, 33, 4195.
23 M. T. Stephan, J. J. Moon, S. H. Um et al., *Nat. Med.*, 2010, 16, 1035.
24 M. T. Stephan, S. B. Stephan, P. Bak et al., Biomaterials, 2012, 33, 5776.
25 T. Heinze, T. Liebert, B. Heublein et al., Functional Polymers Based on Dextran BT - Polysaccharides II, (Eds: D. Klemm), Springer Berlin Heidelberg, Berlin, Germany 2006: 199–291.
26 S. Suarez, G. N. Grover, R. L. Braden et al., *Biomacromolecules*, 2013, 14, 3927.
27 S. L. Suarez, A. Muñoz, A. Mitchell, R. et al., *ACS Biomater. Sci. Eng.*, 2016, 2, 197.
28 H. Uosaki, A. Magadum, K. Seo et al., *Circ. Cardiovasc. Genet.*, 2013, 6, 624.
29 S. Sharma, V. R. Kotamraju, T. Mölder et al., *Nano Lett.*, 2017, 17, 1356.
30 L. Paasonen, S. Sharma, G. B. Braun et al., *Chembiochem.*, 2016, 17, 570.
31 E. Ruoslahti, *Adv. Drug Deliv. Rev.*, 2017, 110–111, 3.
32 J. Hamzah, V. R. Kotamraju, J. W. Seo et al., *Proc. Natl. Acad. Sci. U. S. A.*, 2011, 108, 7154.
33 V. Fogal, L. Zhang, S. Krajewski et al., *Cancer Res.*, 2008, 68, 7210.
34 H. -B. Pang, G. B. Braun, T. Friman et al., *Nat. Commun.*, 2014, 5, 4904.
35 K. J. Kauffman, N. Kanthamneni, S. A. Meenach et al., *Int. J. Pharm.*, 2012, 422, 356.
36 M. Danaei, M. Dehghankhold, S. Ataei et al., Pharmaceutics, 2018, 10, 57.
37 L. Simón-Gracia, P. Scodeller, S. S. Fuentes et al., Oncotarget, 2018, 9, 18682.
38 S. Pabisch, B. Feichtenschlager, G. Kickelbick et al., *Chem. Phys. Lett.*, 2012, 521, 91.
39 L. Kou, J. Sun, Y. Zhai et al., *Asian J. Pharm. Sci.*, 2013, 8, 1.

View Article Online
DOI: 10.1039/C9NR09934D

40 F. B. Engel, M. Schebesta, M. T. Duong et al., *Genes Dev.*, 2005, 19,
41 A. -S. Tseng, F. B. Engel, M. T. Keating, *Chem. Biol.*, 2006, 13, 957.
42 J. F. Callahan, J. L. Burgess, J. A. Fornwald et al., *J. Med. Chem.*, 2002, 45, 999.
43 D. B. Ring, K. W. Johnson, E. J. Henriksen et al., *Diabetes*, 2003, 52, 588.
44 E. M. Bachelder, T. T. Beaudette, K. E. Broaders et al., *J. Am. Chem. Soc.*, 2008, 130, 10494.
45 E. R. Gillies, A. P. Goodwin, J. M. J. Fréchet, *Bioconjug. Chem.*, 2004, 15, 1254.
46 J. L. Cohen, S. Schubert, P. R. Wich et al., *Bioconjug. Chem.*, 2011, 22, 1056.
47 Y. Ahmad Nor, Y. Niu, S. Karmakar et al., *ACS Cent. Sci.*, 2015, 1, 328.
48 M. U. Ghori, B. R. Conway, *Am. J. Pharmacol. Sci.*, 2015, 3, 103.
49 K. Frauke Pistel, A. Breitenbach, R. Zange-Volland et al*., J. Control. Release*, 2001, 73, 7.
50 J. A. Cohen, T. T. Beaudette, J. L. Cohen et al., *Adv. Mater.*, 2010, 22, 3593.
51 H. A. Santos, J. Riikonen, J. Salonen et al., Acta Biomater. 2010, 6, 2721.
52 E. Fröhlich, *Int. J. Nanomedicine*, 2012, 7, 5577.
53 S. -F. Chang, H. -C. Li, Y. -P. Huang et al., *J. Biomed. Sci.*, 2016, 23, 3.
54 A. Haghighat, D. Weiss, M. K. Whalin, et al., *Circulation*, 2007, 115, 2049.
55 Y. Feng, Y. Liang, J. Ren et al., *Kidney Dis.*, 2018, 4, 95.
56 A. M. Vollmar, R. Förster, R. Schultz, *Eur. J. Pharmacol.*, 1997, 319, 279.
57 D. E. Owens, N. A. Peppas, *Int. J. Pharm.*, 2006, 307, 93.
58 Y. Li, M. Kröger, W. K. Liu, Biomaterials, 2014, 35, 8467.
59 C. B. Anders, J. J. Chess, D. G. Wingett et al., *Nanoscale Res. Lett.*, 2015, 10, 448.
60 J. C. Zarif, J. R. Hernandez, J. E. Verdone et al., *Biotechniques*, 2016, 61, 33.
61 S. Mia, A. Warnecke, X. -M. Zhang et al., *Scand. J. Immunol.*, 2014, 79, 305.
62 K. Eske, K. Breitbach, J. Köhler et al., *J. Immunol.* Methods, 2009, 342, 13.
63 L. S. Bisgaard, C. K. Mogensen, A. Rosendahl et al., *Sci. Rep.*, 2016, 6, 35234.
64 K. A. Binnemars-Postma, H. W. M. ten Hoopen, G. Storm et al., Nanomedicine. 2016, 11, 2889.
65 S. A. MacParland, K. M. Tsoi, B. Ouyang et al., ACS Nano. 2017, 11, 2428.
66 Y. Qie, H. Yuan, C. A. von Roemeling et al., Sci. Rep. 2016, 6 26269.
67 J. A. Cooper, *J. Cell Biol.*, 1987, 105, 1473.
68 D. A. Kuhn, D. Vanhecke, B. Michen et al., *Beilstein J. Nanotechnol.*,2014, 5, 1625.
69 S. M. Liu, K. -E. Magnusson, T. Sundqvist, *J. Cell. Physiol.*, 1993, 156, 311.
70 T. dos Santos, J. Varela, I. Lynch et al., *PLoS One*, 2011, 6, e24438.
71 K. H. Sit, B. H. Bay, K. P. Wong, *Vitr. Cell. Dev. Biol. - Anim.*, 1993, 29, 395.
72 L. Thors, J. Eriksson, C. J. Fowler, *Br. J. Pharmacol.*,2007, 152, 744.
73 Z. M. Qian, H. Li, H. Sun et al., *Pharmacol. Rev.*, 2002, 54, 561.
74 M. C. Bennett, G. W. Mlady, Y. -H. Kwon et al., *J. Neurochem.*, 1996, 66, 2606.
75 J. N. Stannard, B. L. Horecker, *J Biol Chem.*, 1948, 172, 599.
76 N. Shrestha, F. Araújo, M. -A. Shahbazi et al., *Adv. Funct. Mater.*, 2016, 26, 3405.

Table of Contents

View Article Online
DOI: 10.1039/C9NR09934D

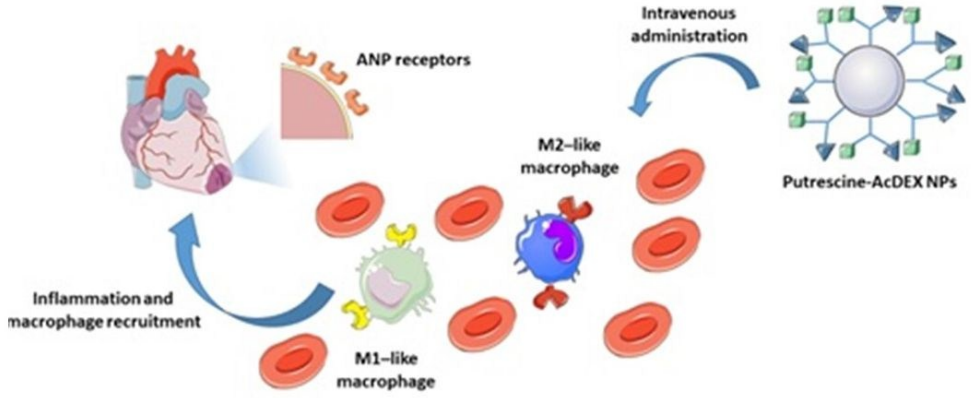

Fabrication of a dual-peptide functionalized acetalated dextran based nanosystem able to exploit the macrophages recruitment occurring during myocardial infarction.